AFFDL-TR-66-80

NUMERICAL APPROACH FOR WAVE MOTIONS IN NONLINEAR SOLID MEDIA

Alfredo H.-S. Ang*

University of Illinois
Urbana, Illinois

The development of a lumped-parameter model of three-space solid media and its important definitions and properties are described. Field problems of solid media can be formulated with reference to the model, resulting in a system of recursive equations which are obtained on the basis of fundamental principles of mechanics and basic material behavior. The equations of the model are also shown to be central finite difference analogues of the differential equations of the corresponding continuum model. Although the model is applicable to many static and dynamic problems of solid media, the application of the approach is illustrated with dynamic problems of wave propagations in spherically and axially symmetric solids.

INTRODUCTION

Initial and/or boundary-value problems of solid media in two and three space dimensions invariably involve great analytical difficulties. These difficulties are necessarily more severe when the idealizations of linear elasticity are removed and material nonlinearity and inelasticity are included in the formulation, and when complete solutions under these realistic conditions are desired. In order to be able to include as many as possible of the physical factors and parameters that constitute a real problem of solid media, a computational approach formulated on the basis of mathematically consistent lumped-parameter models is proposed.

The underlying discrete models can be developed by properly concentrating the masses of elemental volumes at appropriate mass points and defining average strains and stresses for elemental volumes at appropriate stress points. The inertial and deformational equations of a solid medium can then be defined for such a model at the mass points and stress points, respectively; the resulting equations are compatible with the basic requirements of a solid, and are furthermore identical with one of the central finite difference analogues of the differential equations of the corresponding continuous model. In one sense, the model serves to provide a physically meaningful finite difference grid for a solid continuum, and through which initial and/or boundary value problems of solid media can be formulated and solved directly on the basis of simple physical principles of mechanics and material behavior.

Instead of formulating problems on the basis of a continuum model and subsequently reducing the resulting differential equations into finite difference equations by more or less arbitrary rules (or by trial and error), a problem can be formulated in finite mathematical terms directly through the model. The latter approach leads to a system of recurrent equations which are physically meaningful with reference to the model, are also consistently central finite difference analogues of the corresponding continuum equations, and are directly adaptable to high-speed digital calculations. Furthermore, physical boundary conditions present little or no difficulty since these can be included in the recurrent equations simply as imposed displacements or average applied stresses on the appropriate boundary mass points.

*Professor of Civil Engineering

The model and its underlying properties and definitions are described in three-space; however, the solution technique is illustrated for nonlinear-nonelastic solids with specialized geometries. For this latter purpose specialized discrete models are also presented and used for problems involving the numerical prediction of motions or stresses in elastic-perfectly plastic solids possessing spherical and axial symmetry. The details of the calculation technique are described for these special situations, and one problem for each case is illustrated numerically.

DISCRETE MODEL OF 3-SPACE SOLIDS

Basic Definitions and Relations

The proposed discrete model of solid media can be developed within the premise of a few basic and simple definitions. In the rectangular Cartesian system of reference, the model is shown symbolically in Figures 1 and 2. It is composed of two basic types of lumped elements denoted as mass points and stress points; the relative positions of these elements are indicated in Figure 2, and their physical meanings are as follows:

Mass Point -- The total mass of a solid medium is concentrated at the mass points. Each mass point contains the mass of the solid corresponding to an elemental pyramidal volume of $\frac{1}{6}(\Delta x)\,(\Delta y)\,(\Delta z)$. All particle motions (accelerations, velocities, and displacements) of the solid are defined only at the mass points.

Stress Point -- A stress point is the point of definition of the average stress and strain tensors of the solid within an elemental volume of $\frac{1}{6}(\Delta x)\,(\Delta y)\,(\Delta z)$ as indicated in Figure 1; the material in this volume, therefore, is in homogeneous states of stress and strain. The deformability, or conversely the resistance, of a solid medium is represented by the deformability, or resistance, of a finite number of stress points.

In Figures 1 and 2, the stress points are shown symbolically in the form of deformable springs; these are to be considered as generalized axial and shear springs possessing properties identical with whatever behavioral properties are ascribed to a solid. The effective area of a generalized spring is equal to the average area over its length; for instance, the effective area normal to $\sigma_x(i, j, k)$, Figure 1, is equal to,

$$\frac{\frac{1}{6}\,(\Delta x)\,(\Delta y)\,(\Delta z)}{\Delta x} = \frac{1}{6}\,(\Delta y)\,(\Delta z)$$

Within the assumption of infinitesimal strains, all the components of a symmetric strain tensor at a stress point can be derived directly from the model on the basis of purely geometric arguments. Considering a stress point (i, j, k), Figure 1, the strain components are:

$$\epsilon_x(i,j,k) = \frac{u(i+1,j,k) - u(i-1,j,k)}{\Delta x} \tag{1}$$

$$\epsilon_y(i,j,k) = \frac{v(i,j+1,k) - v(i,j-1,k)}{\Delta y} \tag{2}$$

$$\epsilon_z(i,j,k) = \frac{w(i,j,k+1) - w(i,j,k-1)}{\Delta z} \tag{3}$$

$$\gamma_{xy}(i,j,k) = \frac{u(i,j+1,k) - u(i,j-1,k)}{\Delta y} + \frac{v(i+1,j,k) - v(i-1,j,k)}{\Delta x} \tag{4}$$

$$\gamma_{xz}(i,j,k) = \frac{u(i,j,k+1) - u(1,j,k-1)}{\Delta z} + \frac{w(i+1,j,k) - w(i-1,j,k)}{\Delta x} \tag{5}$$

$$\gamma_{yz}(i,j,k) = \frac{v(i,j,k+1) - v(i,j,k-1)}{\Delta z} + \frac{w(i,j+1,k) - w(i,j-1,k)}{\Delta y} \tag{6}$$

The above expressions for the strain components can be recognized to be respectively, central finite difference analogues of the following classical differential expressions for the strain components

$$\epsilon_x = \frac{\partial u}{\partial x}, \quad \epsilon_y = \frac{\partial v}{\partial y}, \quad \epsilon_z = \frac{\partial w}{\partial z}$$

$$\gamma_{xy} = \frac{\partial v}{\partial x} + \frac{\partial u}{\partial y}, \quad \gamma_{xz} = \frac{\partial w}{\partial x} + \frac{\partial u}{\partial z}, \quad \gamma_{yz} = \frac{\partial w}{\partial y} + \frac{\partial v}{\partial z}$$

Equations of Dynamical Equilibrium

The equation of motion of mass point (i,j,k) in the x-direction can be derived on the basis of Newton's second law; thus,

$$\frac{1}{6}(\Delta y)(\Delta z)\left[\sigma_x(i+1,j,k) - \sigma_x(i-1,j,k)\right]$$

$$+\frac{1}{6}(\Delta x)(\Delta z)\left[\tau_{xy}(i,j+1,k) - \tau_{xy}(i,j-1,k)\right]$$

$$+\frac{1}{6}(\Delta x)(\Delta y)\left[\tau_{xz}(i,j,k+1) - \tau_{xz}(i,j,k-1)\right] = \frac{\rho}{6}(\Delta x)(\Delta y)(\Delta z)\,\ddot{u}_o$$

Dividing both sides of the above equation by $\frac{1}{6}(\Delta x)(\Delta y)(\Delta z)$ yields,

$$\frac{\sigma_x(i+1,j,k) - \sigma_x(i-1,j,k)}{\Delta x} + \frac{\tau_{xy}(i,j+1,k) - \tau_{xy}(i,j-1,k)}{\Delta y}$$

$$+\frac{\tau_{xz}(i,j,k+1) - \tau_{xz}(i,j,k-1)}{\Delta z} = \rho\,\ddot{u}_o \qquad (7)$$

Similarly, the equations of motion in the y- and z-directions of mass point (i,j,k) can be shown to be, respectively,

$$\frac{\sigma_y(i,j+1,k) - \sigma_y(i,j-1,k)}{\Delta y} + \frac{\tau_{xy}(i+1,j,k) - \tau_{xy}(i-1,j,k)}{\Delta x}$$

$$+\frac{\tau_{yz}(i,j,k+1) - \tau_{yz}(i,j,k-1)}{\Delta z} = \rho\,\ddot{v}_o \qquad (8)$$

and,

$$\frac{\sigma_z(i,j,k+1) - \sigma_z(i,j,k-1)}{\Delta z} + \frac{\tau_{xz}(i+1,j,k) - \tau_{xz}(i+1,j,k)}{\Delta x}$$

$$+\frac{\tau_{yz}(i,j+1,k) - \tau_{yz}(i,j-1,k)}{\Delta y} = \rho\,\ddot{w}_o \qquad (9)$$

It is easily recognized that Equations 7 through 9 are each, respectively, a central finite difference analogue of the following differential equations of motion of a solid continuum:

$$\frac{\partial \sigma_x}{\partial x} + \frac{\partial \tau_{xy}}{\partial y} + \frac{\partial \tau_{xz}}{\partial z} = \rho \frac{\partial^2 u}{\partial t^2} \tag{10}$$

$$\frac{\partial \sigma_y}{\partial y} + \frac{\partial \tau_{xy}}{\partial x} + \frac{\partial \tau_{yz}}{\partial z} = \rho \frac{\partial^2 v}{\partial t^2} \tag{11}$$

$$\frac{\partial \sigma_z}{\partial z} + \frac{\partial \tau_{xz}}{\partial x} + \frac{\partial \tau_{yz}}{\partial y} = \rho \frac{\partial^2 w}{\partial t^2} \tag{12}$$

The mathematical consistency of the model as indicated above can also be shown for the displacement equations of motion. Consider an isotropic and homogeneous Hookean solid; using Hooke's stress-strain equations in Equation 7 through 9 and applying Equations 1 through 6 for the strain components, the resulting displacement equations of motion in the x, y, and z-directions are thus, respectively, as follows:

$$\begin{aligned} & G\left\{\frac{u(i+2,j,k) - 2u(i,j,k) + u(i-2,j,k)}{(\Delta x)^2} + \frac{u(i,j+2) - 2u(i,j,k) + u(i,j-2,k)}{(\Delta y)^2}\right. \\ & \qquad \left. + \frac{u(i,j,k+2) - 2u(i,j,k) + u(i,j,k-2)}{(\Delta z)^2}\right\} \\ & + (\lambda+G)\left\{\frac{u(i+2,j,k) - 2u(i,j,k) + u(i-2,j,k)}{(\Delta x)^2}\right. \\ & - \frac{[v(i+1,j+1,k) - v(i+1,j-1,k)] - [v(i-1,j+1,k) - v(i-1,j-1,k)]}{(\Delta x)\ (\Delta y)} \\ & \left. + \frac{[w(i+1,j,k+1) - w(i+1,j,k-1)] - [w(i-1,j,k+1) - w(i-1,j,k-1)]}{(\Delta x)\ (\Delta z)}\right\} = \rho\, \ddot{u}_o \end{aligned} \tag{13}$$

$$\begin{aligned} & G\left\{\frac{v(i+2,j,k) - 2v(i,j,k) + v(i-2,j,k)}{(\Delta x)^2} + \frac{v(i,j+2,k) - 2v(i,j,k) + v(i,j-2,k)}{(\Delta y)^2}\right. \\ & \qquad \left. + \frac{v(i,j,k+2) - 2v(i,j,k) + v(i,j,k-2)}{(\Delta z)^2}\right\} \\ & + (\lambda+G)\left\{\frac{[u(i+1,j+1,k) - u(i-1,j+1,k)] - [u(i+1,j-1,k) - u(i-1,j-1,k)]}{(\Delta x)\ (\Delta y)}\right. \\ & \qquad + \frac{v(i,j+2,k) - 2v(i,j,k) + v(i,j-2,k)}{(\Delta y)^2} \\ & \left. + \frac{[w(i,j+1,k) - w(i,j+1,k-1)] - [w(i,j-1,k+1) - w(i,j-1,k-1)]}{(\Delta y)\ (\Delta z)}\right\} = \rho\, \ddot{v}_o \end{aligned} \tag{14}$$

and,

$$G\left\{\frac{w(i+2,j,k) - 2w(i,j,k) + w(i-2,j,k)}{(\Delta x)^2} + \frac{w(i,j+2,k) - 2w(i,j,k) + w(i,j-2,k)}{(\Delta y)^2}\right.$$

$$\left. + \frac{w(i,j,k+2) - 2w(i,j,k) + w(i,j,k-2)}{(\Delta z)^2}\right\}$$

$$+ (\lambda+G)\left\{\frac{[u(i+1,j,k+1) - u(i-1,j,k+1)] - [u(i+1,j,k-1) - u(i-1,j,k-1)]}{(\Delta x)(\Delta z)}\right.$$

$$+ \frac{[u(i,j+1,k+1) - v(i,j-1,k+1)] - [v(i,j+1,k-1) - v(i,j-1,k-1)]}{(\Delta y)(\Delta z)}$$

$$\left. + \frac{w(i,j,k+2) - 2w(i,j,k) + w(i,j,k-2)}{(\Delta z)^2}\right\} = \rho\, \ddot{w}_o \qquad (15)$$

where λ and G are the Lame's constants, and ρ is the mass density of the solid. Equations 13 through 15 can again be recognized to be, respectively, central finite difference analogues of the following displacement differential equations of an isotropic Hookean solid continuum:

$$G\left(\frac{\partial^2 u}{\partial x^2} + \frac{\partial^2 u}{\partial y^2} + \frac{\partial^2 u}{\partial z^2}\right) + (\lambda+G)\cdot\left(\frac{\partial^2 u}{\partial x^2} + \frac{\partial^2 v}{\partial x \partial y} + \frac{\partial^2 w}{\partial x z}\right) = \rho\,\frac{\partial^2 u}{\partial t^2} \qquad (16)$$

$$G\left(\frac{\partial^2 v}{\partial x^2} + \frac{\partial^2 v}{\partial y^2} + \frac{\partial^2 v}{\partial z^2}\right) + (\lambda+G)\cdot\left(\frac{\partial^2 u}{\partial x \partial y} + \frac{\partial^2 v}{\partial y^2} + \frac{\partial^2 w}{\partial y \partial z}\right) = \rho\,\frac{\partial^2 v}{\partial t^2} \qquad (17)$$

$$G\left(\frac{\partial^2 w}{\partial x^2} + \frac{\partial^2 w}{\partial y^2} + \frac{\partial^2 w}{\partial z^2}\right) + (\lambda+G)\cdot\left(\frac{\partial^2 u}{\partial x \partial z} + \frac{\partial^2 v}{\partial y \partial z} + \frac{\partial^2 w}{\partial t^2}\right) = \rho\,\frac{\partial^2 w}{\partial t^2} \qquad (18)$$

It may be emphasized that the equations of dynamical equilibrium are defined for all the mass points. Furthermore, since all components of the strain and strain rate tensors and of the associated stress and stress rate tensors are defined at a stress point, the constitutive equations of a material are sufficiently defined for each stress point within the basic assumptions of the model.

Boundary Conditions

By consistently applying the basic definitions and average properties of the model at its boundary, the two types of boundary conditions can be defined accordingly for the model. Effectively, a stress boundary condition is defined at the fictitious stress points immediately outside of the boundary mass points, while a displacement boundary condition is defined by specifying the required displacements of the mass points on the boundary.

In the process of numerical solution, any displacement boundary condition must be included in the strain-displacement equations, Equations 1 through 6, for the appropriate stress points, and any stress boundary condition must be included in the dynamical equations of equilibrium, Equations 7 through 9, of the appropriate boundary mass points.

Significance of the Model

The proposed discrete model of solid media is developed on the premise of the definition of certain average physical quantities at specified points in the solid. This leads to a model whose average properties are in every respect consistent with those of an idealized solid element, and are also compatible with the basic theories of elasticity and plasticity. Furthermore, the equations of the model which can be derived on the basis of fundamental principles of mechanics are also consistently a central finite difference analogue of the differential equations of the corresponding continuum model. Because of this latter attribute of the model, mathematical theories of finite differences, such as domain of dependence inequalities of hyperbolic systems of equations, may be used with the model to ensure stable calculations.

The model is intended to provide a discrete model of solid media from which a finite mathematical formulation of problems of deformable solids can be obtained directly on the basis of fundamental principles of mechanics and basic physical behavior of materials. Such a formulation leads directly to a system of recursive equations which are intuitively meaningful and are readily adaptable to high-speed machine calculations. Because the inherent simplicity and physical clarity of the approach holds equally well for nonlinear-nonelastic materials as it does for linearly elastic material, the use of the discrete model embodies a somewhat unified numerical approach to the analysis of solid media.

Statement of Basic Problem

A field problem of solid media can be considered as that of determining the motions and states of strain and stress of the lumped-parameter model under appropriate boundary conditions. The basic problem is then the determination of the six components of the strain tensors and the corresponding components of the associated stress tensors at all stress points plus the three components of the displacement vectors at all mass points in the model. For a model consisting of n mass points and n stress points, there are 15n unknowns as follows: $\epsilon_x, \epsilon_y, \epsilon_z$, $\gamma_{xy}, \gamma_{xz}, \gamma_{yz}$; σ_z $\tau_{xy}, \tau_{xz}, \tau_{yz}$ at the n stress points and u, v, w at the n mass points. Equations 1 through 6 for the n stress points and Equation 7 through 9 for the n mass points represent a system of 9n equations; the additional 6n equations must be furnished by the constitutive equations of the material at the n stress points.

A solution of the basic problem stated above may be accomplished by numerical methods of calculation, wherein the equations of the model and the appropriate material equations are used recursively in the numerical process. Specific problems of spherically symmetric and axially symmetric solids and the appropriate solution techniques are illustrated in the sequel.

SPHERICALLY SYMMETRIC ELASTIC-PLASTIC PROBLEM

For a spherically symmetric solid, the discrete model is reduced appropriately in spherical coordinates, to that of Figure 3, where all physical quantities are functions only of the radial distance, r and time, t. For illustration, a problem of a contained explosion in an infinite solid is considered as shown in Figure 4. The material is assumed to be an elastic-perfectly plastic solid in which the material at any stress point obeys Hooke's linear stress-strain equations prior to any yielding as given by the von Mises yield condition. Thereafter the material obeys the Prandtl-Reuss elastic-plastic equations. Unloading from a plastic state is governed by the rate form of Hook's equations. The pressure pulse shown in Figure 5 is applied uniformly over the surface of a spherical cavity in the solid. Zero initial conditions are assumed of the solid.

Recursive Equations for Spherically-Symmetric Solids

With reference to Figure 3, the recursive equations for solids with spherical symmetry are as follows:

Strain-Displacement Relations:

$$\epsilon_r^t(i) = \frac{u^t(i+1) - u^t(i-1)}{\Delta r} \tag{19}$$

$$\epsilon^t(i) = \epsilon_\theta^t(i) = \frac{u^t(i)}{r(i)} \tag{20}$$

The finite model is terminated at a radius of r = 4.72a (i = 160) with the following boundary conditions,

$$u^t(160) = 0$$

$$\dot{u}^t(160) = 0$$

Equations of Dynamical Equilibrium:

$$\ddot{u}^t(i) = \frac{1}{\rho}\left[\frac{\sigma_r^t(j+1) - \sigma_r^t(i-1)}{\Delta r} + \frac{2\sigma_r^t(i) - 2\sigma^t(i)}{r(i)}\right] \tag{21}$$

where, for the problem in Figure 4, the stress boundary conditions are,

$$\sigma_r^t(0) = p(t)$$

Material Equations (Elastic-Perfectly Plastic):

All quantities are for stress point i at time t.

When

$$J_2 \equiv \frac{1}{3}(\sigma_r - \sigma_\varphi)^2 < k_o^2 \tag{22}$$

$$\sigma_r = 3\lambda e + 2G\epsilon_r$$

$$\sigma_\varphi = 3\lambda e + 2G\epsilon_\varphi$$

where

$$e = \epsilon_r + 2\epsilon_\varphi$$

$$k_o = \text{yield limit in simple shear} \tag{23}$$

when

$$J_2 = k_o^2 \text{ and } \dot{W} = \frac{2}{3}(\sigma_r - \sigma_\varphi)(\dot{\epsilon}_r - \dot{\epsilon}_\varphi) > 0,$$

$$\dot{\sigma}_r = K(\dot{\epsilon}_r + 2\dot{\epsilon}_\varphi) \tag{24}$$

$$\dot{\sigma}_\varphi = \dot{\sigma}_r \tag{25}$$

where K is the bulk modulus.

When $J_2 = k_o^2$ and $\dot{W} \leq 0$, unloading from a plastic state commences at stress point i; elastic unloading is assumed and the rate form of Equation 22 and 23 are used.

Quadrature Relations

For static or quasi-static problems, $\ddot{u} = 0$ for all mass points; Equations 19 through 25 therefore, represent a set of recursive relations which are sufficient for determining the unknowns in the problem. Iterative techniques may then be used to obtain the required solutions as has been done previously for an elastic-plastic plane problem (Reference 1).

For dynamical problems, the following quadrature relations are used in a step-by-step marching process: (Reference 2)

$$\dot{u}^{t+\Delta t}(i) = \dot{u}^{t}(i) + \frac{\Delta t}{2}\left[\ddot{u}^{t+\Delta t}(i) + \ddot{u}^{t}(i)\right] \tag{26}$$

$$u^{t+\Delta t}(i) = u^{t}(i) + (\Delta t)\,\dot{u}^{t}(i) + \frac{(\Delta t)^2}{2}\,\ddot{u}^{t}(i) \tag{27}$$

Numerical Integration Process

Assuming that all physical quantities are known at time t, the corresponding quantities at time $t + \Delta t$ are obtained by using the above recursive equations iteratively. The sequence of calculations within one cycle of calculations consists of the following steps:

(1) Calculate $\ddot{u}^{t+\Delta t}(i)$ from Equation 21

(2) From the results of (1), calculate $\dot{u}^{t+\Delta t}(i)$ and $u^{t+\Delta t}(i)$.

(3) From the results of (2), calculate the strain and strain rate components at all stress points.

(4) On the basis of the states of strain and stress at time t, stress points i are examined to determine the applicable material equations for each stress point.

(5) Calculate stress rates and total stresses at all stress points using appropriate material equations (Equations 22 and 23 or Equations 24 and 25) for each stress point.

(6) Recalculate $\ddot{u}^{t+\Delta t}(i)$ with new stresses in Equation 21 and repeat steps (1) through (5) if necessary.

Stability Requirements

In the above numerical process of integration, the time and space meshes used in the computational scheme must satisfy certain requirements necessary for stable calculations. For spherical wave propagation in an elastic medium, one of the conditions for stable finite difference calculations (Reference 3), known as the Courant condition, is

$$\Delta t \leq \frac{\Delta r}{c_1} \tag{28}$$

where $c_1 = \sqrt{\frac{\lambda+2G}{\rho}}$, the elastic dilatational velocity of propagation. In the elastic-plastic range of behavior, the propagation velocity of the plastic pulse is less than c_1, hence Equation 28 is still valid.

For reliable reproduction of pressure pulses, it has been shown empirically (Reference 4) for one-dimensional plane wave propagation that the space mesh must be chosen with respect to the minimum rise or decay time, t_r, of the applied pressure pulse as follows:

$$\Delta x \leq \frac{c}{\pi} t_r \tag{29}$$

where

$$c = \sqrt{\frac{E}{\rho}}$$

For spherical wave propagation, the condition,

$$\Delta r \leq \frac{c_1}{\pi} t_r \tag{30}$$

has also proved to yield reliable results.

The accuracy of the calculation technique is illustrated in Figure 6 in which elastic results obtained with the numerical technique are compared with the corresponding results obtained from an analytic solution (Reference 5).

Results of Elastic-Plastic Calculations

Numerical solution from the calculations of a problem with $k_0 = p_0/7$ and $\frac{c_2}{c_1} = 0.753$ (where $c_2 = \sqrt{K/\rho}$) are presented, in the form of histories in Figures 7 through 10. For purposes of comparison, corresponding results for the related elastic problem are also shown in the same figure in dash curves.

The solutions were obtained with a model of uniform mesh lengths $\Delta r = \frac{a}{43}$. The calculation time for the elastic-plastic problem was approximately 5 minutes, while for the corresponding elastic problem, the time was less than 2 minutes on an IBM 7094 machine.

AXI-SYMMETRIC ELASTIC-PLASTIC PROBLEMS

In Figure 11 the discrete model is presented in spherical-polar coordinates for solids with axial symmetry (Reference 6). In this case, all physical quantities are functions of r and ϕ, and time t. For illustration, consider the problem depicted in Figure 12, which is a half-space subjected to a pressure pulse (Figure 13) applied at the surface of a crater (Reference 7). The material is assumed to be an elastic-perfectly plastic solid. Because of axial symmetry, the number of unknowns are reduced from that of the general solid, and the appropriate recursive equations for this model are as follows:

Strain-Displacement Equations:

$$\epsilon_r^t(i,j) = \frac{u^t(i+1,j) - u^t(i-1,j)}{\Delta r} \tag{31}$$

$$\epsilon_{\varphi}^{t}(i,j) = \frac{w^{t}(i,j+1) - w^{t}(i,j-1)}{r(i,j) \cdot \Delta\varphi} + \frac{u^{t}(i,j)}{r(i,j)} \tag{32}$$

$$\epsilon_{\theta}^{t}(i,j) = \frac{u^{t}(i,j)}{r(i,j)} - \frac{w^{t}(i,j)}{r(i,j)} \tan \varphi(i,j) \tag{33}$$

$$\gamma_{r\varphi}^{t}(i,j) = \frac{u^{t}(i,j+1) - u^{t}(i,j-1)}{r(i,j) \cdot \Delta\varphi} + \frac{w^{t}(i+1,j) - w^{t}(i-1,j)}{\Delta r} - \frac{w^{t}(i,j)}{r(i,j)} \tag{34}$$

Equations of Dynamical Equilibrium:

$$\ddot{u}^{t}(i,j) = \frac{1}{\rho}\left[\frac{\sigma_{r}^{t}(i+1,j) - \sigma_{r}^{t}(i-1,j)}{\Delta r} + \frac{\tau_{r\varphi}^{t}(i,j+1) - \tau_{r\varphi}^{t}(i,j+1)}{r(i,j) \cdot \Delta\varphi} + \frac{2\sigma_{r}^{t}(i,j) - \sigma_{\varphi}^{t}(i,j) - \sigma_{\theta}^{t}(i,j) - \tau_{r\varphi}^{t}(i,j) \tan \varphi(i,j)}{r(i,j)}\right] \tag{35}$$

$$\ddot{w}^{t}(i,j) = \frac{1}{\rho}\left[\frac{\sigma_{\varphi}^{t}(i,j+1) - \sigma_{\varphi}^{t}(i,j-1)}{r(i,j) \cdot \Delta\varphi} + \frac{\tau_{r\varphi}^{t}(i+1,j) - \tau_{r\varphi}^{t}(i-1,j)}{\Delta r} + \frac{3\tau_{r\varphi}^{t}(i,j) + \sigma_{\theta}^{t}(i,j) \tan \varphi(i,j) - \sigma_{\varphi}^{t}(i,j) \tan \varphi(i,j)}{r(i,j)}\right] \tag{36}$$

The stress boundary conditions for the problem of Figure 12 are as follows:

$$\sigma_{r}^{t}(0,j) = p(t)$$

$$\tau_{r\varphi}^{t}(0,j) = 0$$

and,

$$\sigma_{\varphi}^{t}(i,0) = 0$$

$$\tau_{r\varphi}^{t}(i,0) = 0$$

And for the purpose of approximating a semi-infinite half-space, the finite model is terminated at a radius of 1140 ft. (i = 33) with the following boundary conditions,

$$\sigma_{r}^{t}(34,j) = 0$$

$$\tau_{r\varphi}^{t}(34,j) = 0$$

Material Equations (Elastic-Perfectly Plastic):

All quantities are for stress point (i,j) at time t.

When $$J_2 \equiv \frac{1}{2}(s_r^2 + s_\varphi^2 + s_\theta^2 + 2\tau_{r\varphi}^2) < k_o^2$$

$$\sigma_r = 3\lambda e + 2G\epsilon_r \tag{37}$$

$$\sigma_\varphi = 3\lambda e + 2G\epsilon_\varphi \tag{38}$$

$$\sigma_\theta = 3\lambda e + 2G\epsilon_\theta \tag{39}$$

$$\tau_{r\varphi} = G\gamma_{r\varphi} \tag{40}$$

where $$e = \frac{1}{3}(\epsilon_r + \epsilon_\varphi + \epsilon_\theta),$$

$$s_r = \sigma_r - \sigma;\ s_\varphi = \sigma_\varphi - \sigma;\ s_\theta = \sigma_\theta - \sigma$$

$$\sigma = \frac{1}{3}(\sigma_r + \sigma_\varphi + \sigma_\theta)$$

When $$J_2 = k_o^2, \text{ and } \dot{W} = s_r\dot{\epsilon}_r + s_\varphi\dot{\epsilon}_\theta + \tau_{r\varphi}\dot{\gamma}_{r\varphi} > 0$$

$$\dot{\sigma}_r = 2G(\dot{\epsilon}_r - \frac{\dot{W}}{2k_o^2} s_r) + 3K\dot{e} \tag{41}$$

$$\dot{\sigma}_\varphi = 2G(\dot{\epsilon}_\varphi - \frac{\dot{W}}{2k_o^2} s_\varphi) + 3K\dot{e} \tag{42}$$

$$\dot{\sigma}_\theta = 2G(\dot{\epsilon}_\theta - \frac{\dot{W}}{2k_o^2} s_\theta) + 3K\dot{e} \tag{43}$$

$$\dot{\tau}_{r\varphi} = 2G(\dot{\gamma}_{r\varphi} - \frac{\dot{W}}{2k_o^2} \tau_{r\varphi}) \tag{44}$$

When $J_2 = k_o^2$ and $\dot{W} \leq 0$, unloading from a plastic state commences at (i,j.), and the rate form of Equations 37 through 40 are used.

Quadrature Relations:

All quantities refer to mass point (i,j).

$$\dot{u}^{t+\Delta t} = \dot{u}^t + \frac{\Delta t}{2}(\ddot{u}^t + \ddot{u}^{t+\Delta t}) \tag{45}$$

$$\dot{w}^{t+\Delta t} = \dot{w}^t + \frac{\Delta t}{2}(\ddot{w}^t + \ddot{w}^{t+\Delta t}) \tag{46}$$

and,

$$u^{t+\Delta t} = u^t + \Delta t\, \dot{u}^t + \frac{(\Delta t)^2}{2} \ddot{u}^t \tag{47}$$

$$w^{t+\Delta t} = w^t + \Delta t\, \dot{w}^t + \frac{(\Delta t)^2}{2} \ddot{w}^t \tag{48}$$

Typical Numerical Results

Certain results of numerical calculations for an elastic-plastic half-space and for the corresponding elastic half-space solid are presented in Figures 14 through 19. The elastic-plastic solid is assumed to have a yield strength of k_o = 10 ksi, while the applied pressure pulse, Figure 13, has a peak pressure of 71 ksi. In Figures 14 and 16, the histories of two stress components along the surface of the half-space are presented; in Figures 15 and 17 the same components along the center line are given. The contours shown in Figure 18 represent maximum radial stresses attained in the solid, and Figure 19 shows the positions of the moving plastic-elastic interface in the half-space as a function of time.

Only typical results of certain stress components can be presented; however, a complete solution consists of the histories of all stress components at all stress points, and the components of all acceleration, velocity, and displacement vectors of all mass points.

Calculation time for the elastic problem was approximately 10 minutes, while the elastic-plastic problem required approximately 30 minutes of calculation on an IBM 7094 computer.

ACKNOWLEDGMENTS

The results presented herein are parts of continuing research programs being conducted in the Department of Civil Engineering at the University of Illinois. These programs have been supported by the National Science Foundation under Grant NSF-GP984, and by the Air Force Weapons Laboratory under Contract AF 29(601)-5851.

Solutions to the problems of axially symmetric solids were obtained by Dr. J. H. Rainer, Assistant Professor of Civil Engineering, and the numerical calculations for the spherically symmetric problems were performed by Mr. G. C.-Y. Chang, Research Assistant in Civil Engineering. Their fine contributions to the paper are acknowledged.

REFERENCES

1. Ang, A. H.-S., and Harper, G. N. "Analysis of Contained Plastic Flow in Plane Solids," Proc. ASCE, Vol. 90, EM5, pp. 397-418, October 1964.

2. Newmark, N. M., "Methods of Computation for Structural Dynamics," Proc. ASCE, Vol. 85, pp. 67-94, July 1959.

3. Rakhmatulin, H. A., and Demyanov, Y. A., Strength of Materials Subjected to Rapid High Intensity Loading, Moscow, 1961 (In Russian).

4. Smith, R. H., and Newmark, N. M., "Numerical Integration for One Dimensional Stress Waves," Structural Research Series No. 162, University of Illinois C. E. Studies, 1958.

5. Ang, A. H.-S., Rainer, J. H., Merritt, J. L., and Newmark, N. M., Solutions of Directly Transmitted and Air-Induced Ground Effects by Digital Simulation, Final Report to United Aircraft Corp. Systems Center, September 1964 (Appendix by A. R. Robinson).

6. Ang, A. H.-S., and Rainer, J. H., "Model for Wave Motions in Axi-Symmetric Solids," Proc. ASCE, Vol. 90, EM2, pp. 195-223, April 1964.

7. Rainer, J. H., Numerical Calculation of Axi-Symmetric Elastic-Perfectly Plastic Wave Motions, Ph.D. Thesis, University of Illinois, 1965.

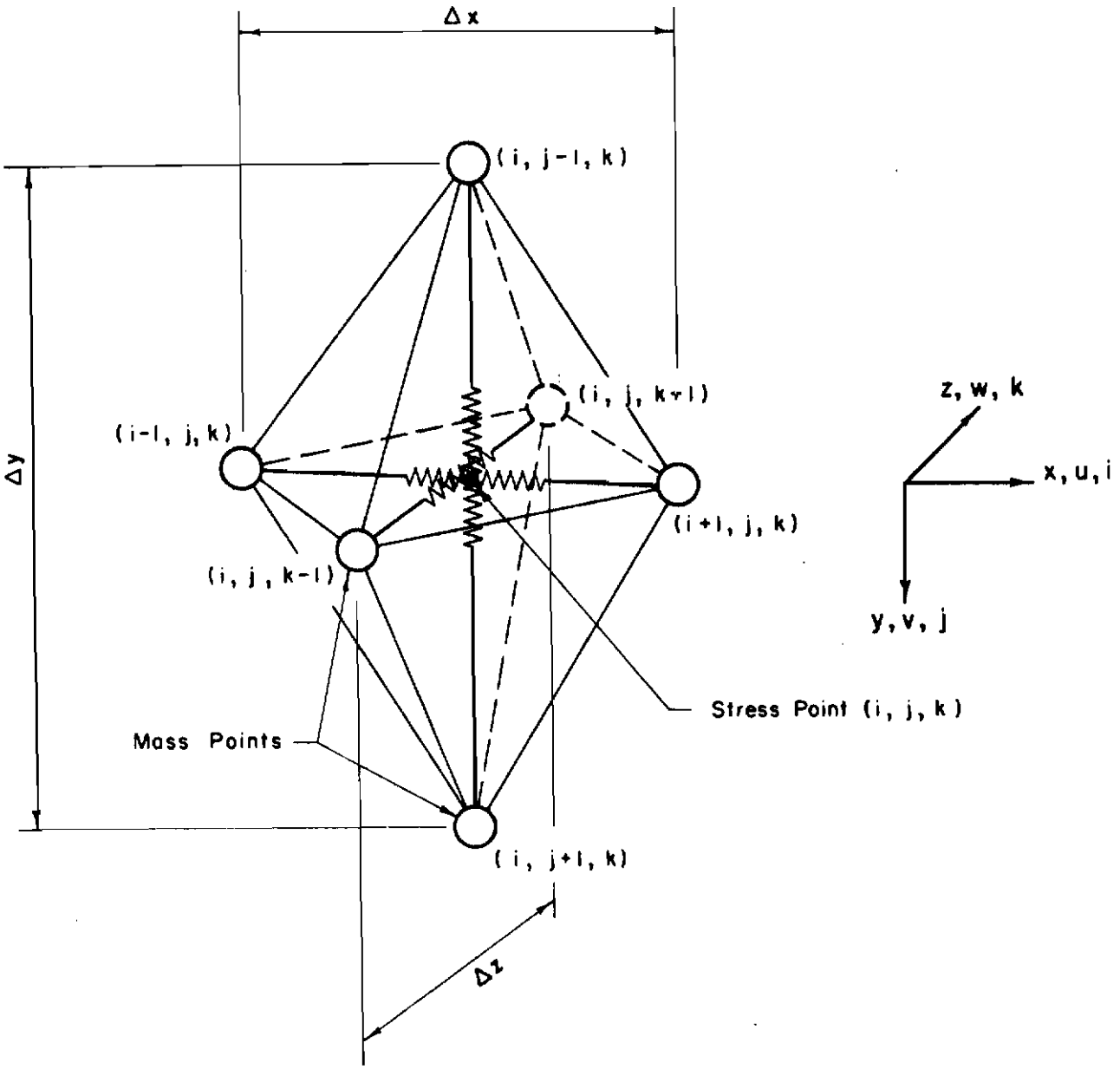

Figure 1. Basic Discrete Element of 3-Space Model

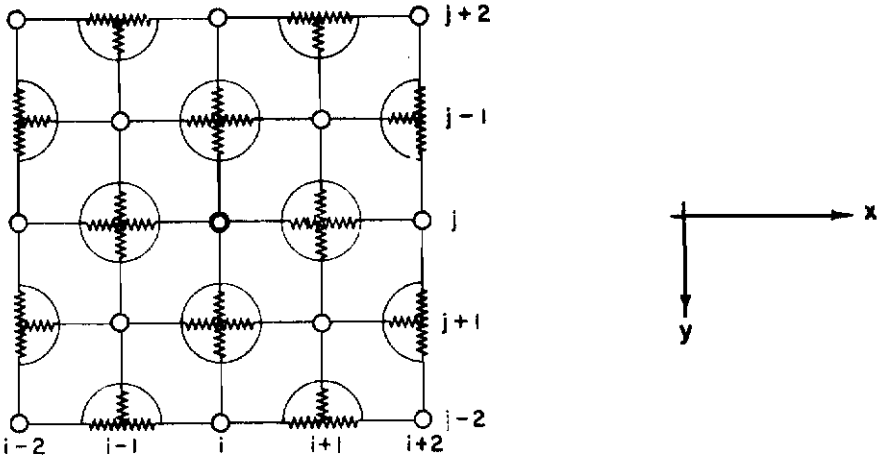

a. Plane x-y of Model (viewed in + z-direction)

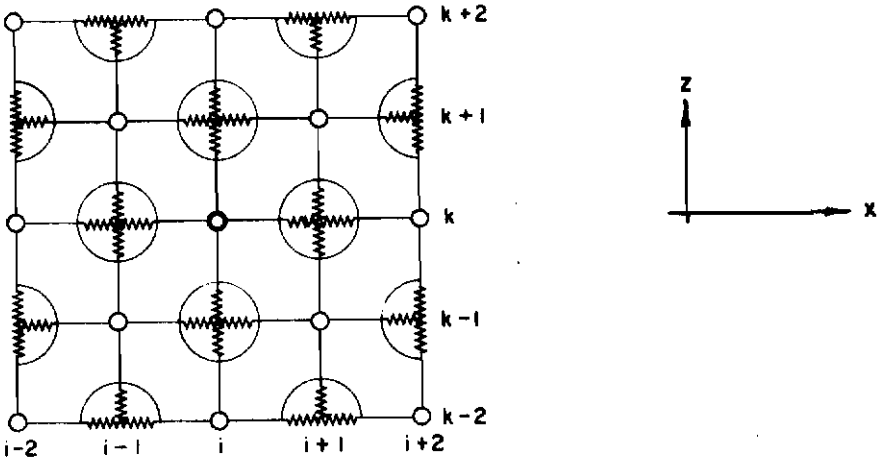

b. Plane x-z of Model (viewed in + y-direction)

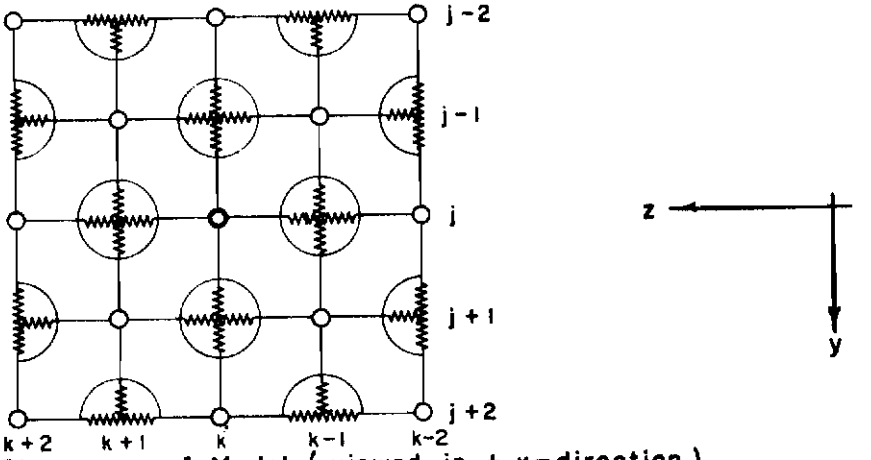

c. Plane y-z of Model (viewed in + x-direction)

Figure 2. Sections of 3-Space Model

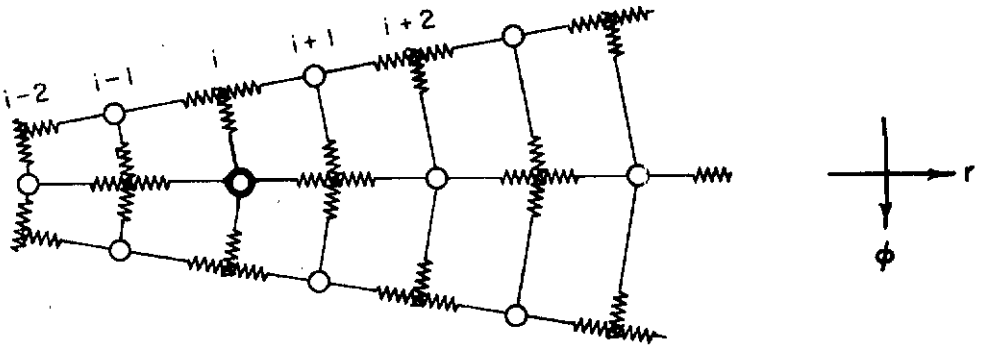

Figure 3. Spherically Symmetric Model

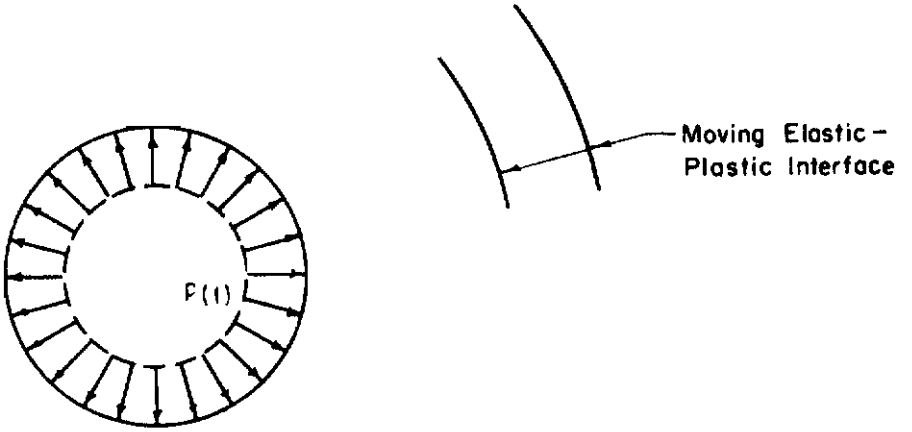

Figure 4. A Spherically Symmetric Full-Space

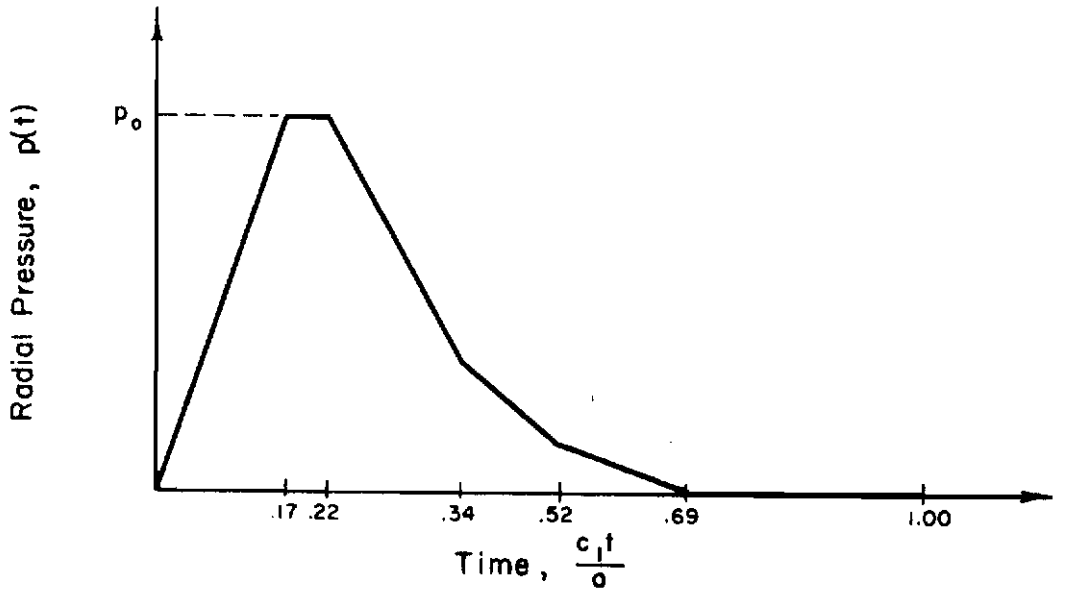

Figure 5. Applied Pressure Pulse

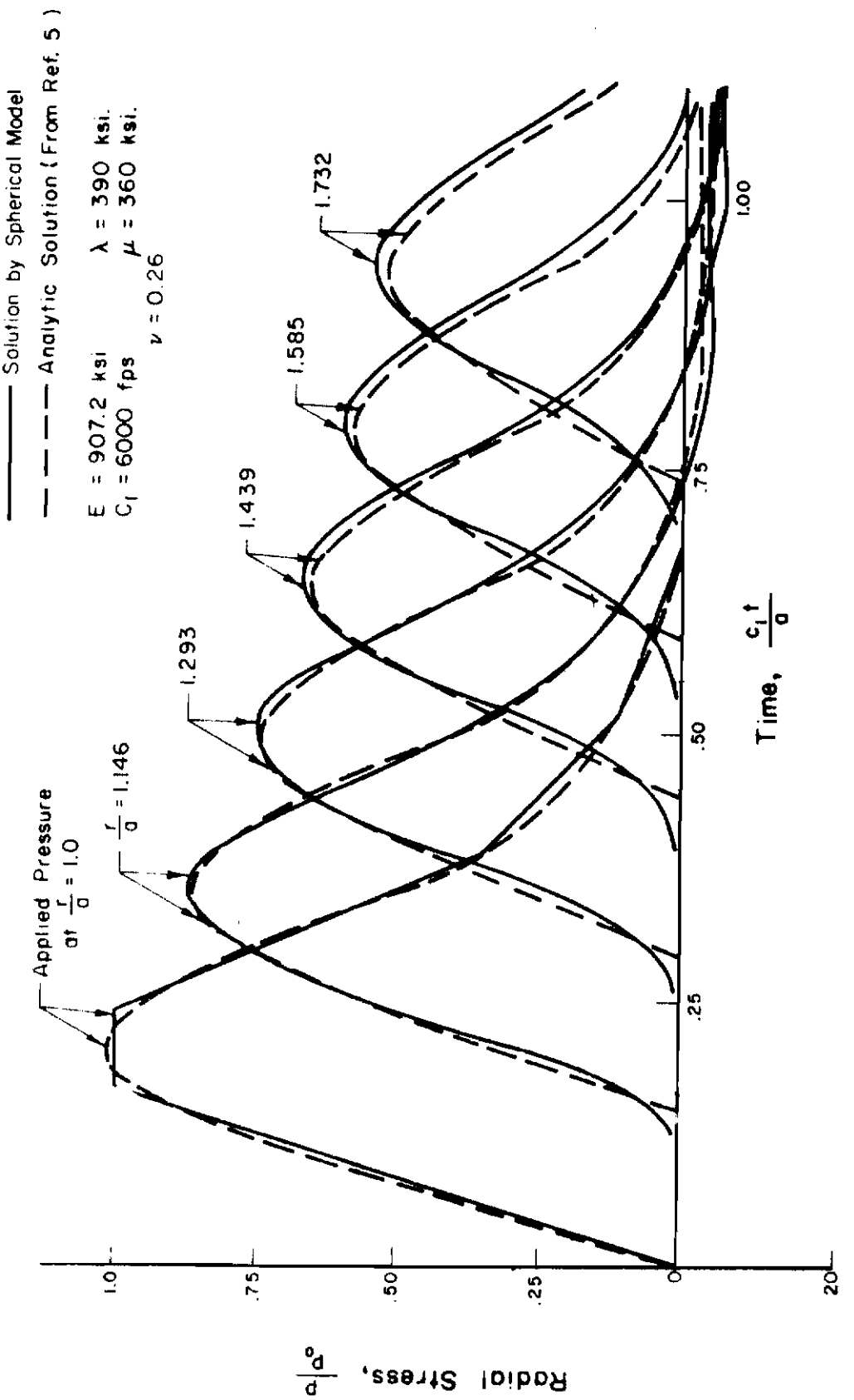

Figure 6. Radial Stresses In Spherically Symmetric Elastic Solid

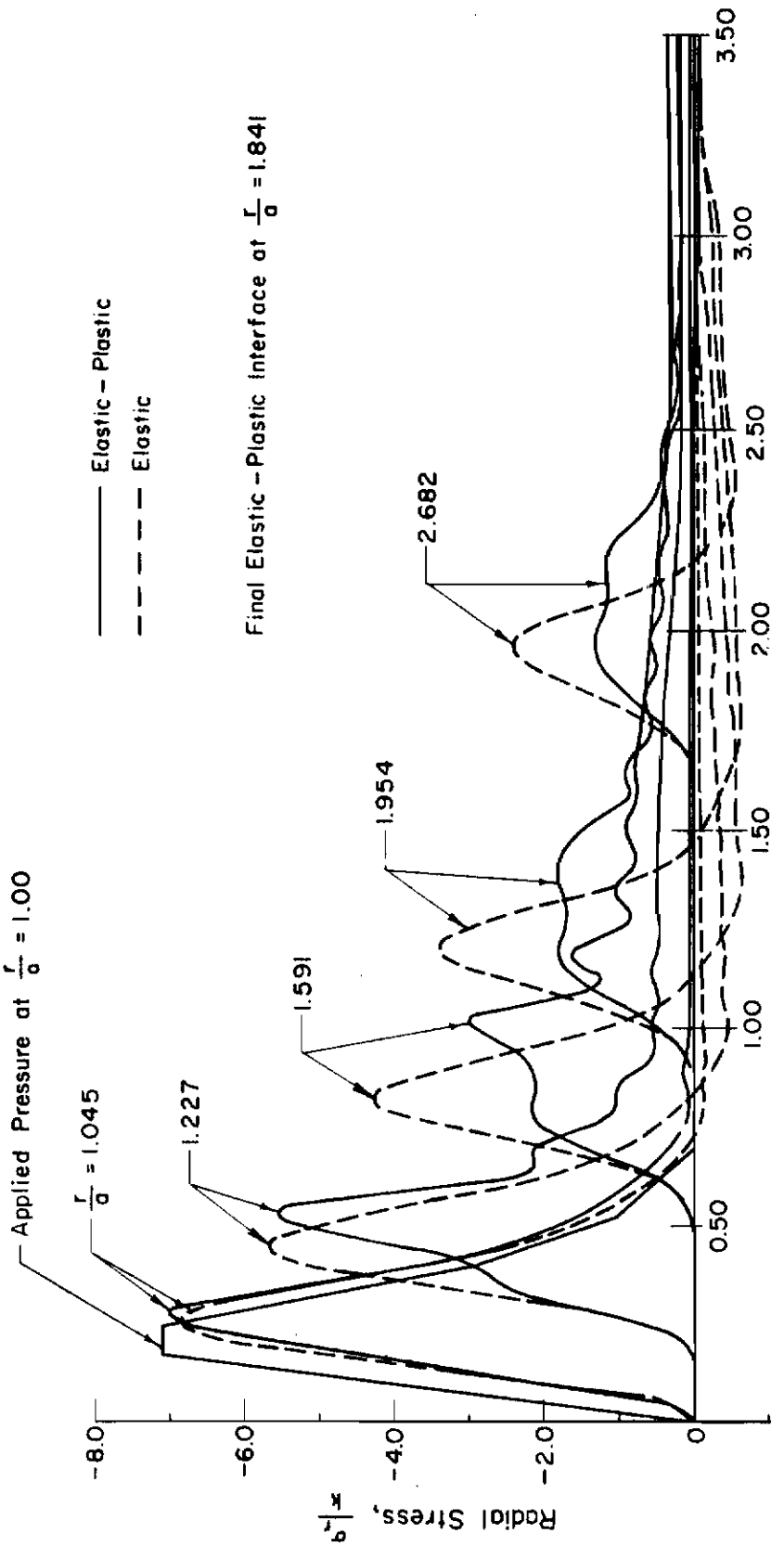

Figure 7. History of Radial Stresses, $k = \frac{\rho_0}{\gamma}, \frac{c_2}{c_1} = 0.753$

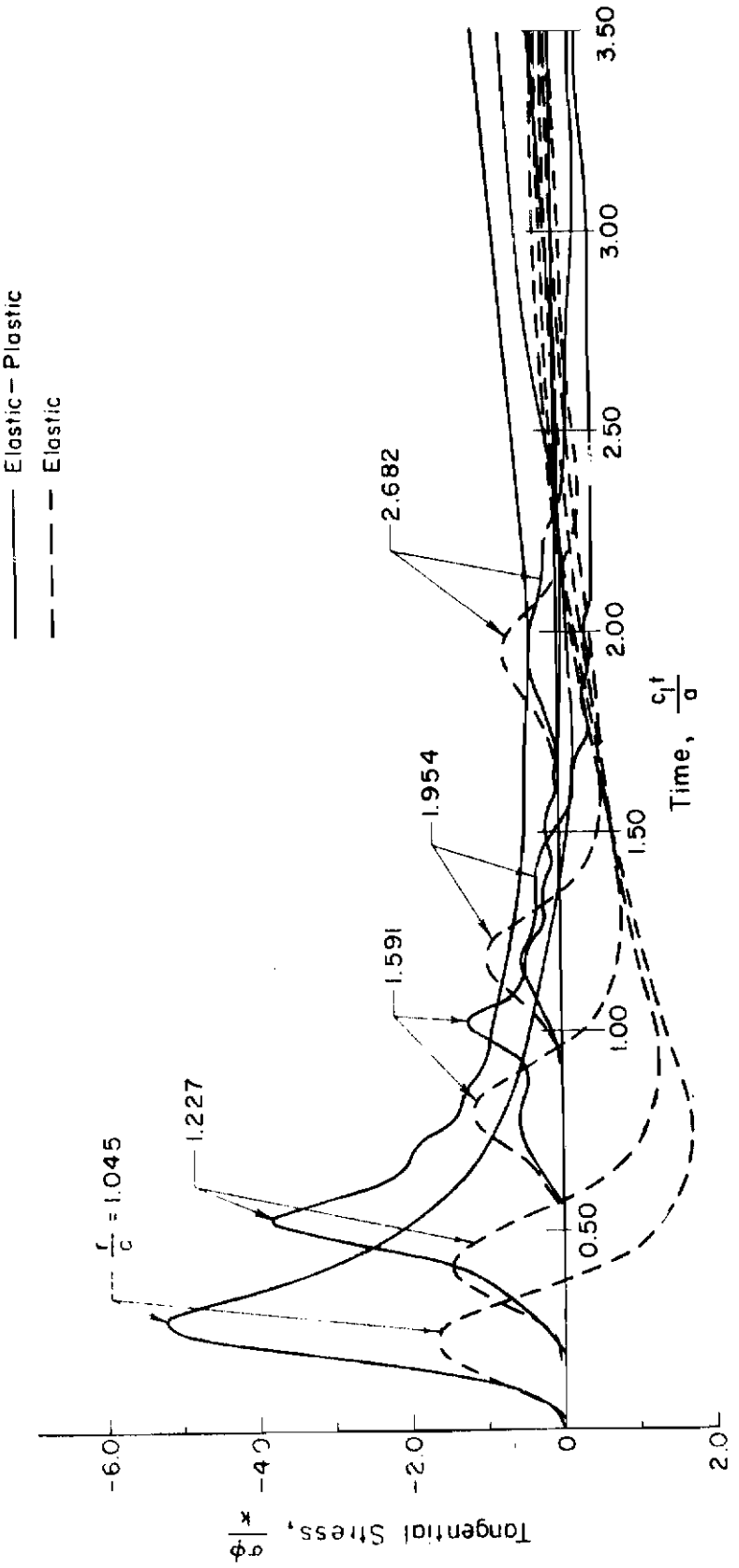

Figure 8. History of Tangential Stresses, $k = \frac{\rho_0}{7}, \frac{c_2}{c_1} = 0.753$

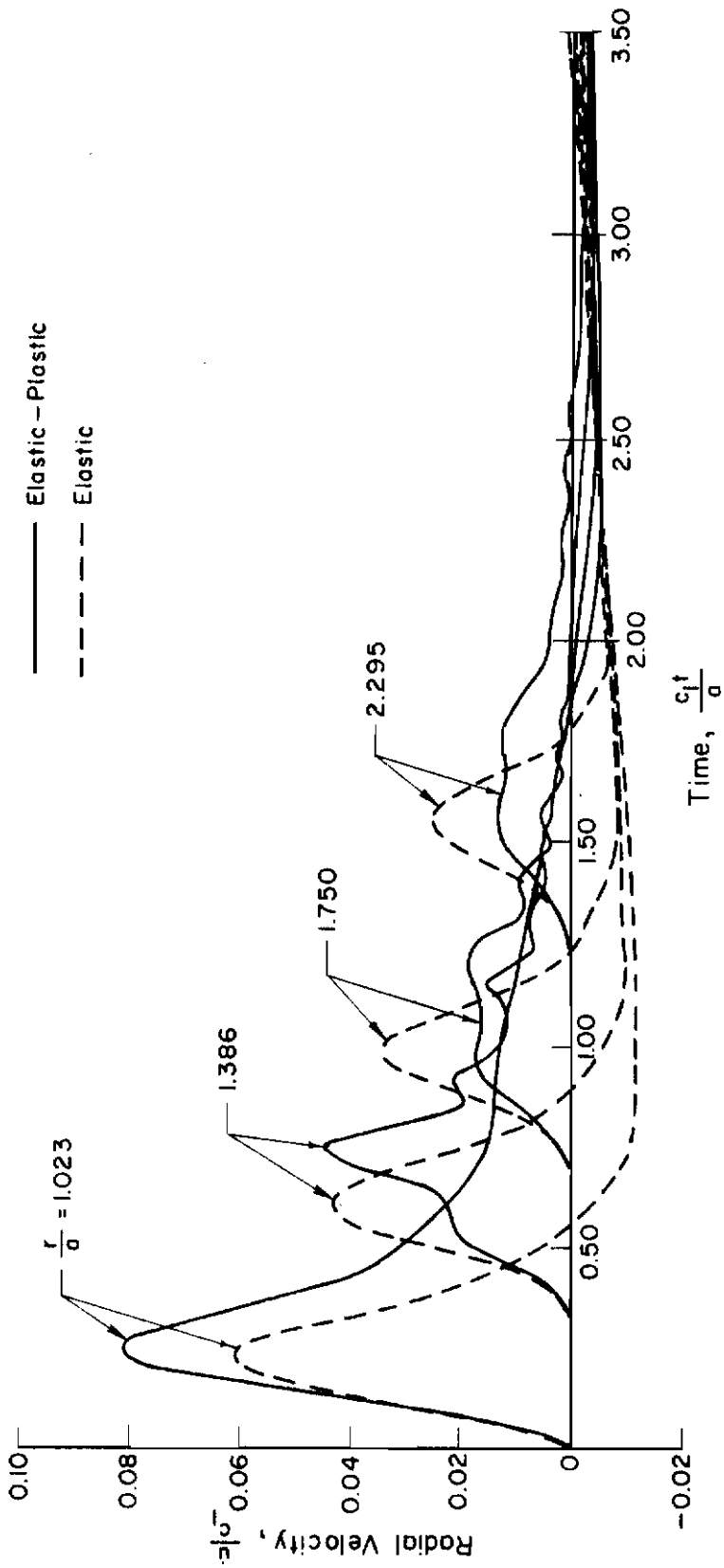

Figure 9. History of Radial Particle Velocities, $k = \frac{p_o}{\gamma}, \frac{c_2}{c_1} = 0.753$

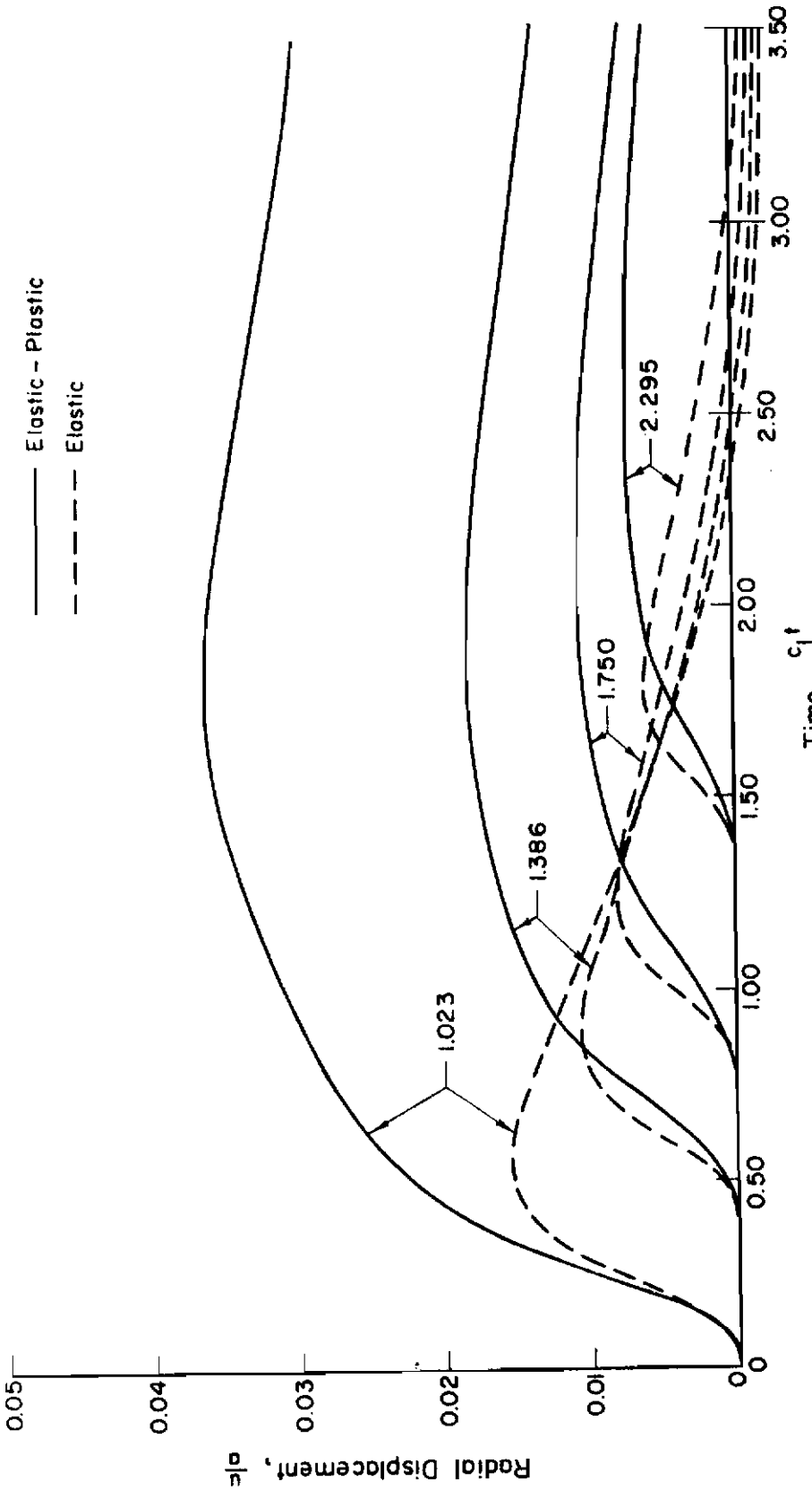

Figure 10. History of Radial Particle Displacement, $k = \frac{\rho_2}{\rho_1}, \frac{c_2}{c_1} = 0.753$

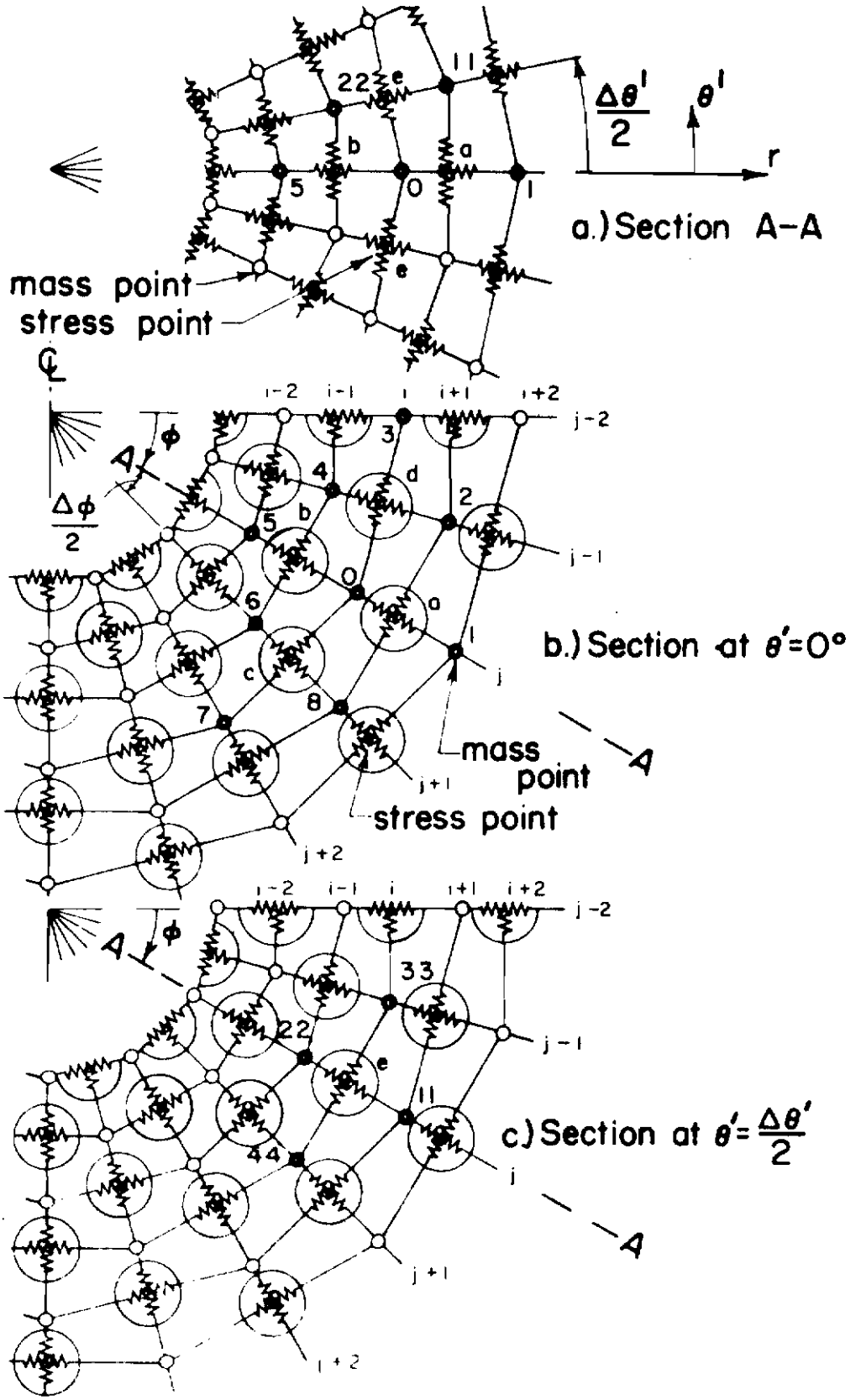

Figure 11. Axially Symmetric Model in Spherical-Polar Coordinates

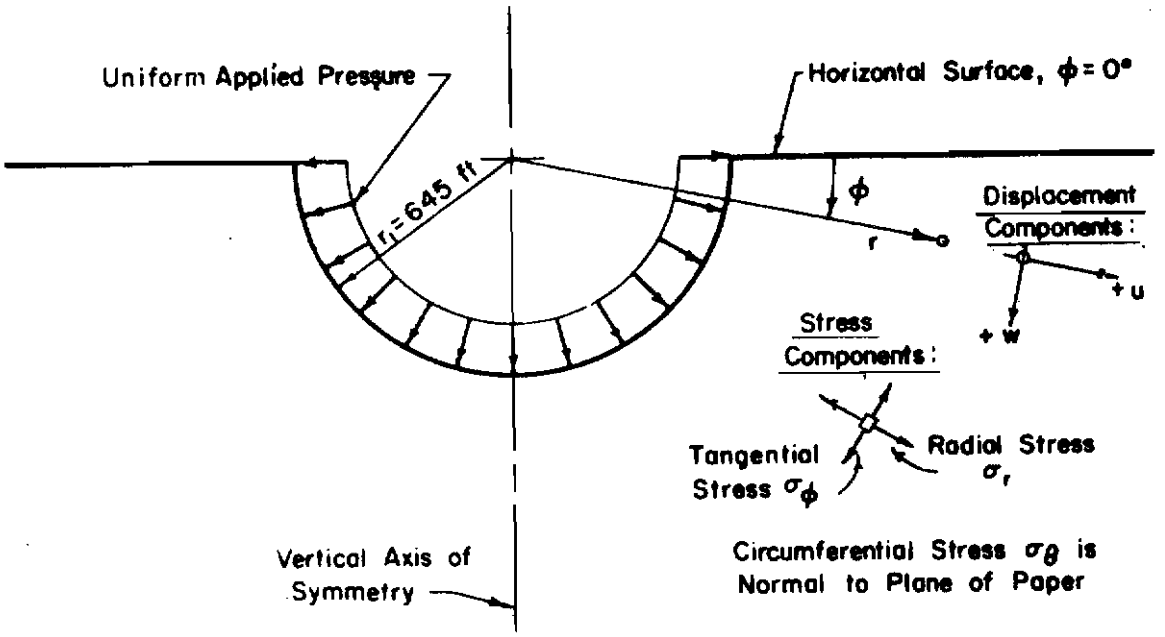

Figure 12. Section Through Elastic-Plastic Half-Space With Semi-Spherical Cavity and Uniform Pressure

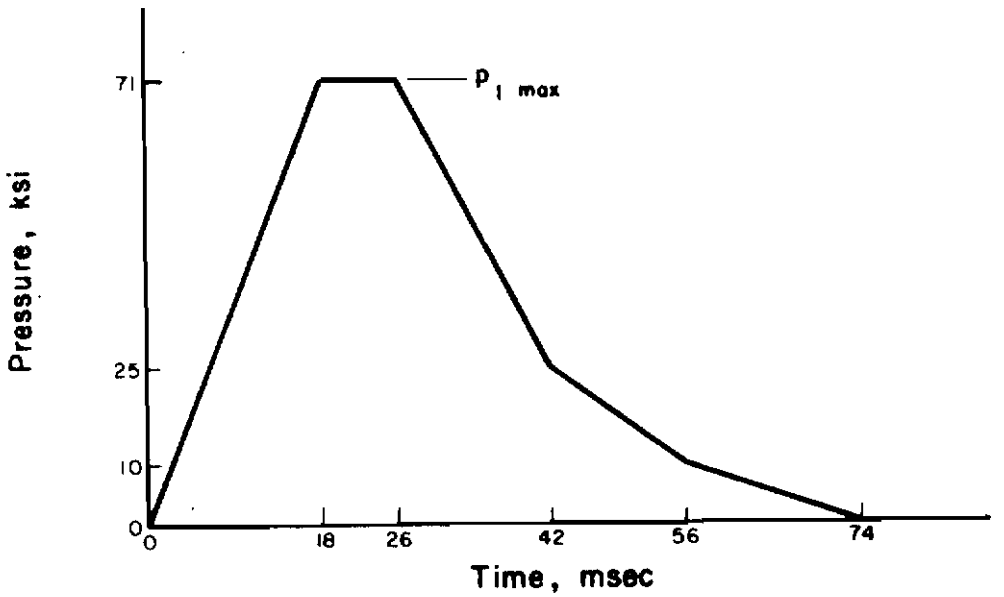

Figure 13. Pressure Pulse Applied To Semi-Spherical Cavity (Uniform Distribution)

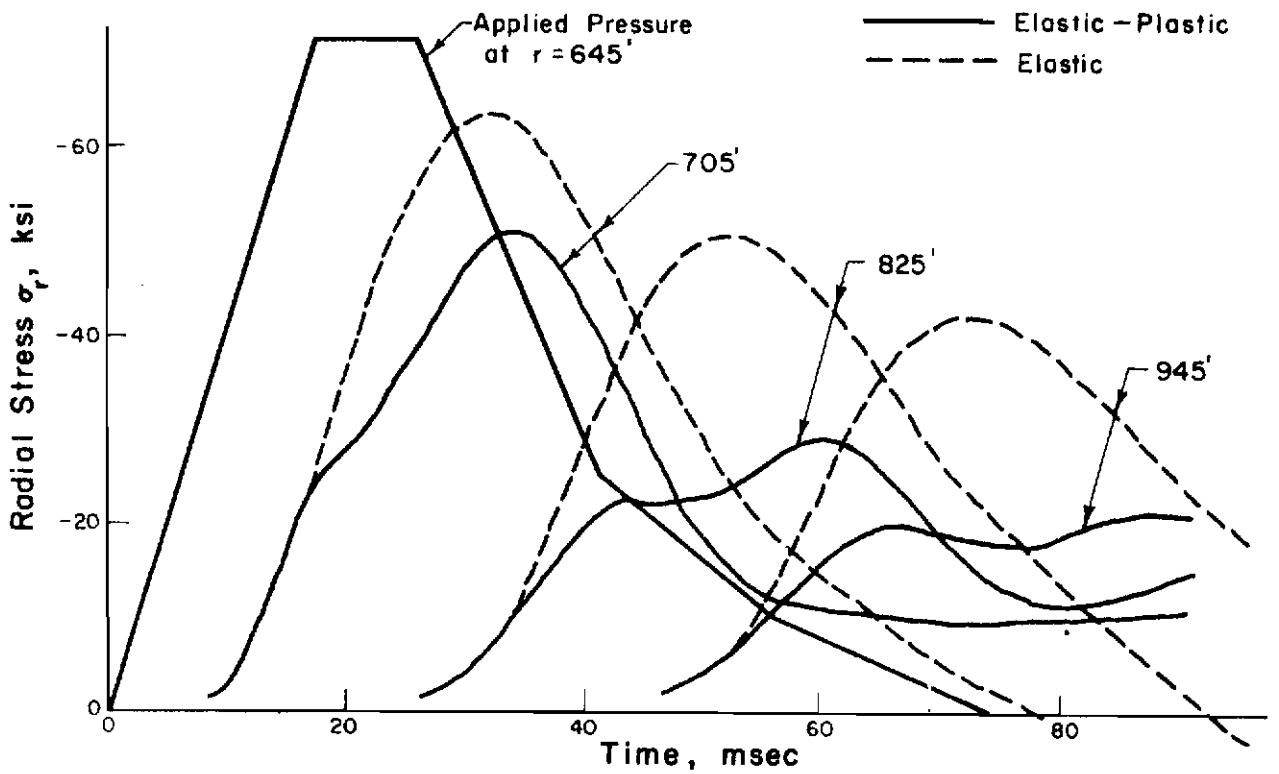

Figure 14. Radial Stresses Along $\phi = 3.75°$ (Surface) For $k_o = 10$ ksi

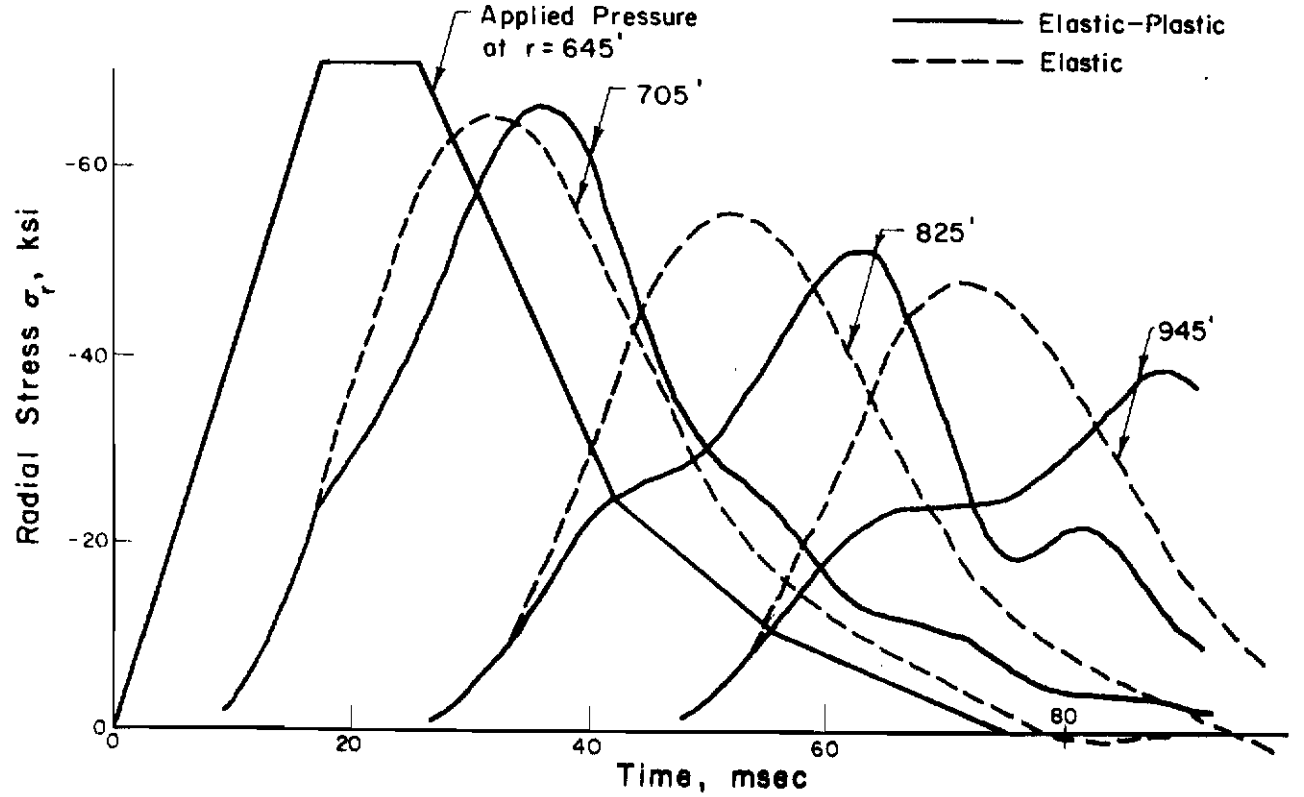

Figure 15. Radial Stresses Along Vertical Axis For $k_o = 10$ ksi

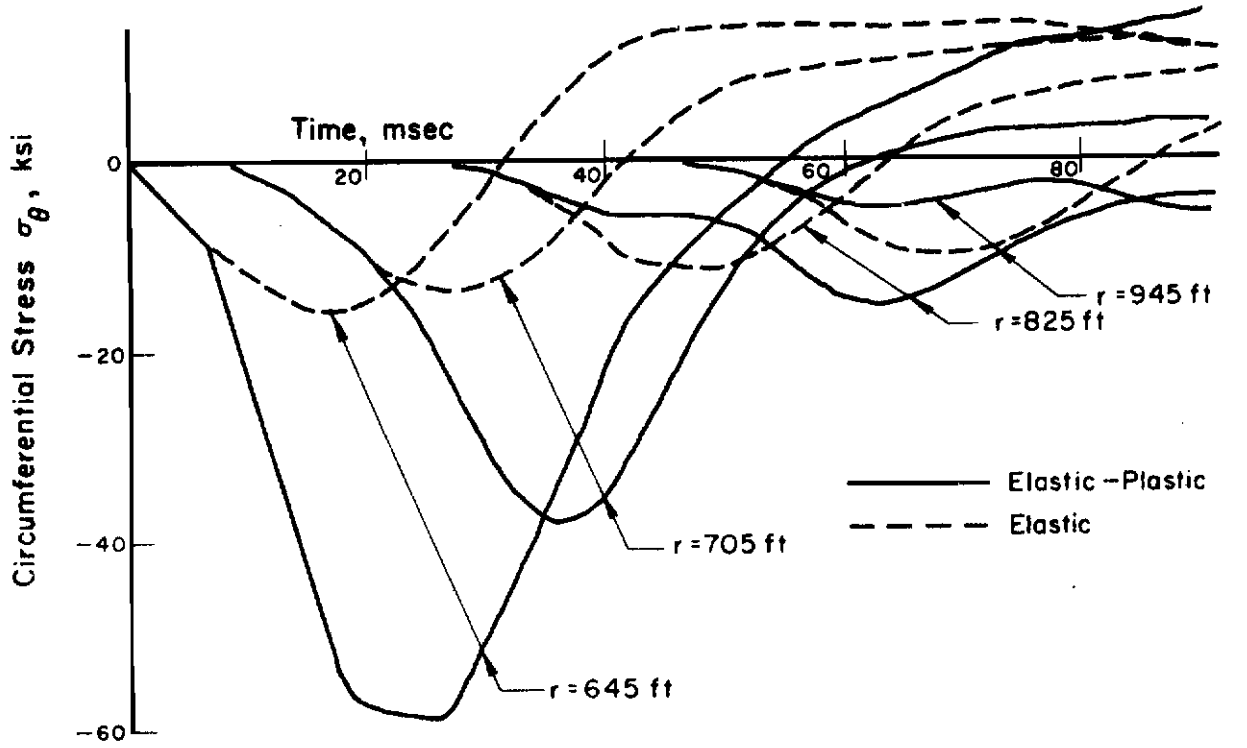

Figure 16. Circumferential Stresses Along ϕ = 3.75° (Surface) For k_o = 10 ksi

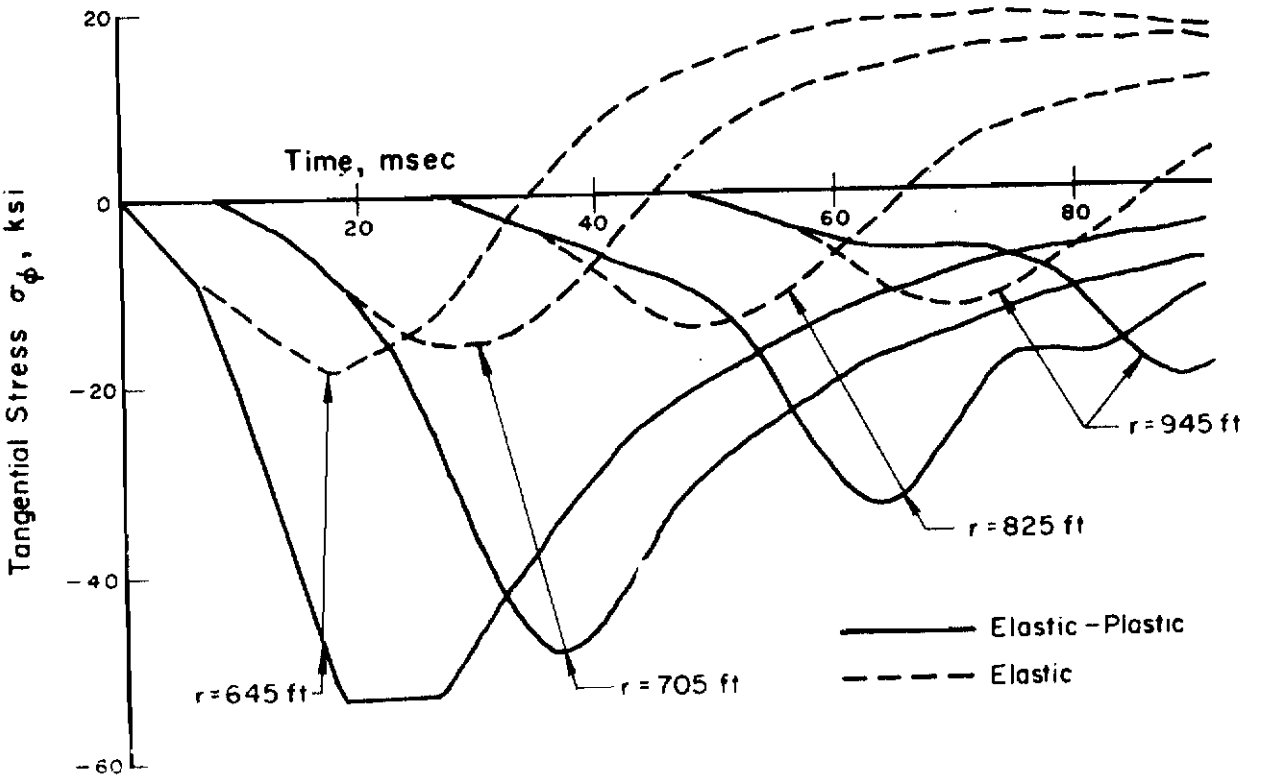

Figure 17. Tangential Stresses Along Vertical Axis For k_o = 10 ksi

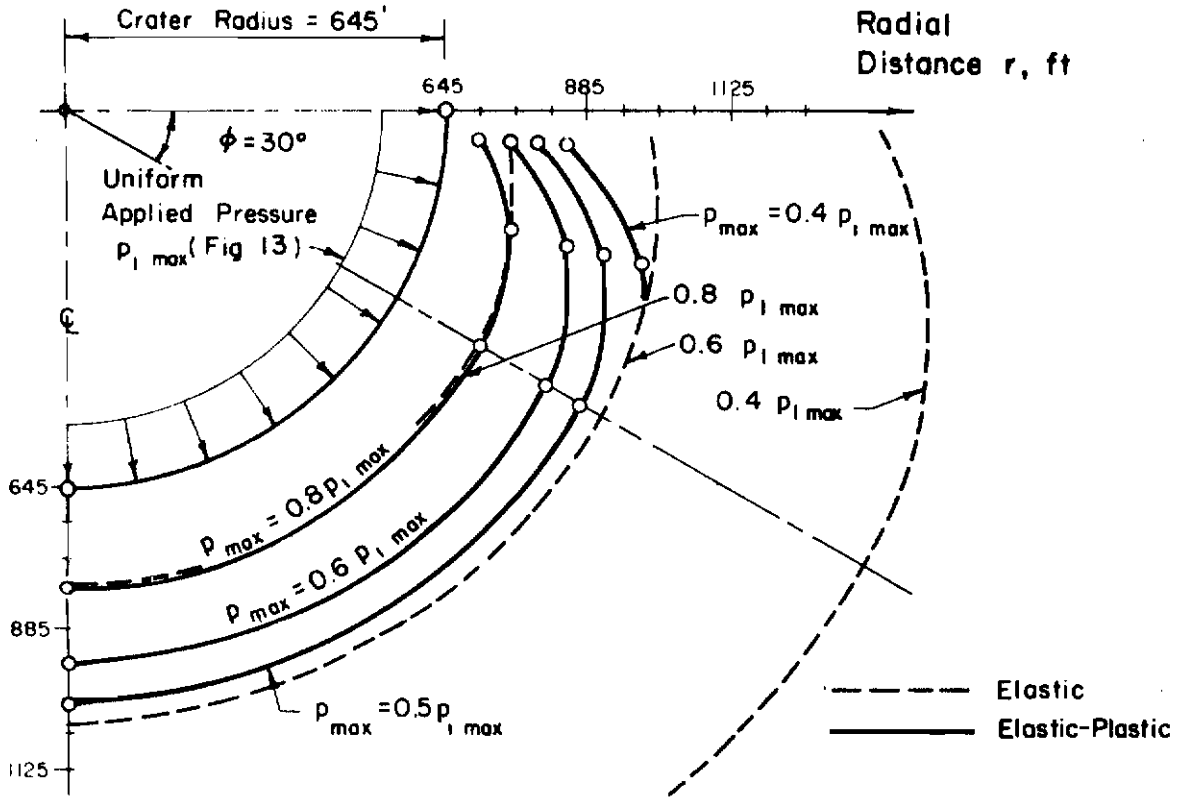

Figure 18. Maximum Radial Stress Contours, k_o = 10 ksi

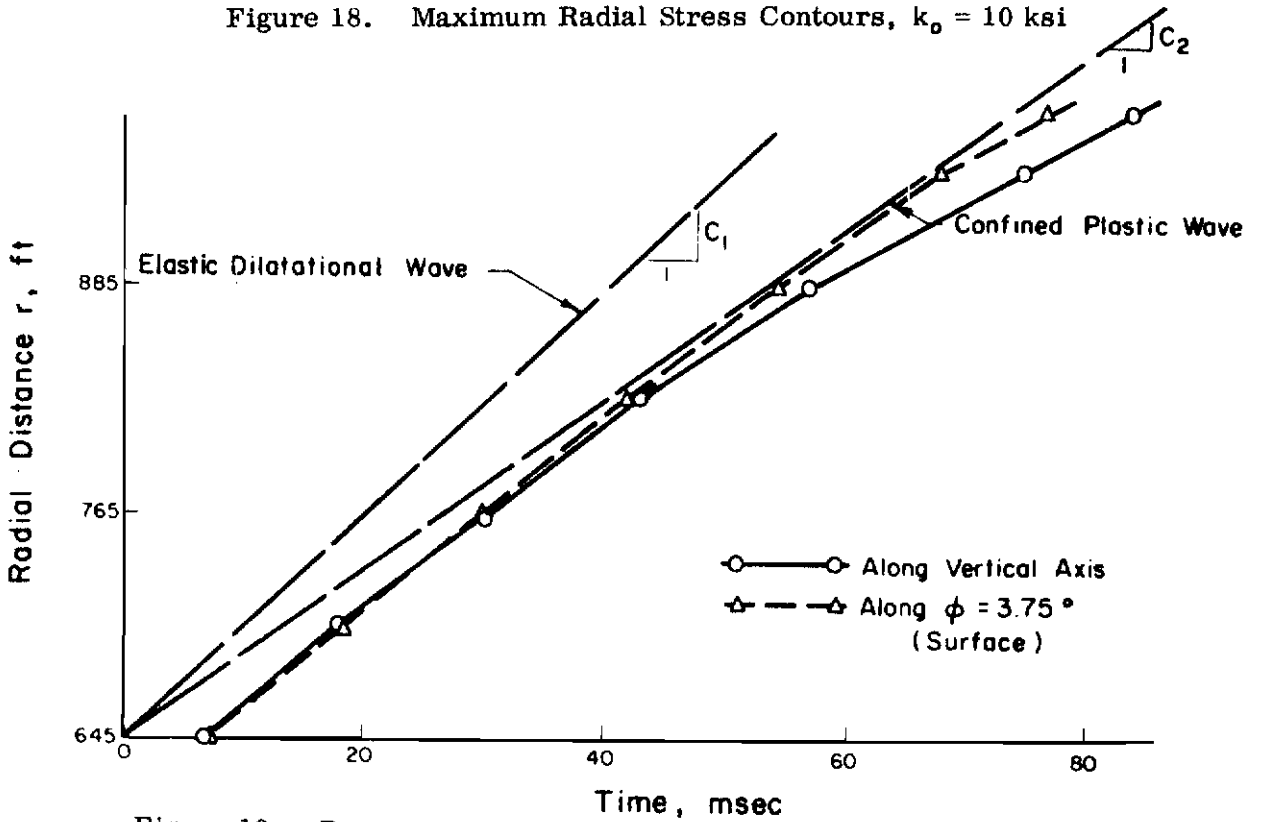

Figure 19. Progression of Elastic-Plastic Interface For k_o = 10 ksi (Uniform Cavity Pressure)